ELSEVIER

Polymer 41 (2000) 5819–5828

polymer

Miscibility studies of erucamide (13-*cis*-docosenamide)/ poly(laurolactam) (nylon 12) (PA-12) blends

M. Fernández de Velasco-Ruiz, I. Quijada-Garrido, R. Benavente, J.M. Barrales-Rienda*

Departamento de Química-Física de Polímeros, Instituto de Ciencia y Tecnología de Polímeros, Consejo Superior de Investigaciones Científicas, Juan de la Cierva, 3, E-28006 Madrid, Spain

Received 22 June 1999; received in revised form 20 September 1999; accepted 5 October 1999

Abstract

A series of erucamide (13-*cis*-docosenamide) and poly(laurolactam) (PA-12) blends have been studied by means of differential scanning calorimetry (DSC), wide-angle X-ray scattering (WAXS) and dynamic mechanical thermal analysis (DMTA). The blends presented three very well differentiated types of behaviour to temperature depending on the erucamide content. Thus, for the lower erucamide content blends (0–6%), they show a good compatibility. For these samples, erucamide (*ERU III*) is dissolved in the amorphous regions of PA-12, which now may be identified as "*melt-like or liquid-like amorphous component*", decreasing the α-relaxation temperature (T_g) of PA-12. In this case the additive acts as a plasticiser. For blends with an erucamide content higher than about 6 wt%, erucamide (*ERU II*) crystallises in the amorphous regions of PA-12, which have a segmental mobility in between those of the crystalline and the liquid-like amorphous component, as proved by the low-temperature endotherm that appears in the DSC traces. This may be a "*disordered phase of anisotropic nature*". Both types of amorphous regions can be considered as interphase components with similar characteristics to the liquid-like and crystalline components, respectively. They act as two true and different matrices with respect to the additive: one as a miscible and homogeneous mixture and the other as crystals dispersed in an amorphous phase. And for blends with still higher erucamide content, a part is segregated and crystallised as pure erucamide (*ERU I*) in the whole polymer matrix as microdomains or droplets.

Keywords: Erucamide (13-*cis*-docosenamide); Poly(laurolactam) (nylon 12); Erucamide/poly(laurolactam) blends

1. Introduction

During the last decade, there has been a large increase in the use of plastic materials for food packaging. Among them, polyamides are extensively used because of their excellent gas barrier properties in conjunction with their satisfactory mechanical properties. Aliphatic polyamides, namely, nylons 11 and 12 differ from polyethylene by having amide groups which give rise to hydrogen bonding between the molecular chains. These intermolecular hydrogen bonds influence strongly the thermomechanical properties of these polyamides.

The diffusion behaviour of erucamide (subsequently referred as eru), a slip and antiblocking additive, in i-PP and in PA-12 was investigated in previous papers [1–3]. For the diffusion of eru in i-PP, a non-Fickian behaviour was found in opposite to the Fickian one found when eru diffused in PA-12. This different behaviour was explained by considering morphological and thermodynamic aspects of these two systems. The equilibrium solubility C_0 and diffusion coefficient D values were also different when comparing both systems. Higher C_0 and lower values of D were found when eru diffused through PA-12. The higher C_0 could be explained by a better compatibility between eru and PA-12. A good compatibility has to be expected since both components incorporate amide groups as well as long methylene sequences in their chemical structures.

Whereas the behaviour of erucamide/i-PP blends was studied in detail by Quijada-Garrido et al. [4–6], the characteristics of erucamide/PA-12 blends remained to be investigated. Erucamide/i-PP showed the typical characteristics of incompatible substances; one of the most relevant features of the mixtures was eru crystallised in the amorphous regions of i-PP. A relationship could be established between the amount of this eru and the amount of amorphous regions in i-PP.

Solubility of small molecules in polymers is a complex process that is controlled by the free volume of the polymer, the size and shape of the additive, and the polymer–additive

* Corresponding author. Tel.: +34-91-562-2900; fax: +34-91-564-4853.
E-mail address: ictbr69@fresno.csic.es (J.M. Barrales-Rienda).

0032-3861/00/$ - see front matter
PII: S0032-3861(99)00769-7

thermodynamic interactions [7–11]. In semicrystalline systems, it is known that solvent molecules are located at the amorphous regions. Although there has been a large development in this field, the state of these small molecules in the amorphous regions is not completely understood. Information about the local incompatibility and the state of the two components in the blend can be obtained by determining the glass transition and some other relaxations [4].

Hudson et al. [12] found for a poly(aryletheretherketone)/poly(etherimide) (PEEK/PEI) blend that the rejection from the crystals may depend upon the relative rates of solvent diffusion and growth of polymer crystals. Three modes of rejection were found. The substance may be rejected completely ahead of the growing front between spherulites, trapped in pockets between lamellar bundles and may also be rejected between individual lamellae. A more complicated picture is expected when the solvent is not an amorphous substance but it is able to crystallise. Inside the amorphous regions, the additive may be located in different places, which possesses different mobility and/or different structure. The state of the additive may be conditioned by its location and by its interactions with the polymeric matrix. The amorphous phase, in a semicrystalline polymer with a low glass transition temperature like PA-12, may be represented by a "*melt-like or liquid-like component*" and a component with a segmental mobility between those of the crystalline and the liquid-like components, known as "*intermediate component or disordered phase of anisotropic nature*" [13]. Thus, for instance, the existence of the "intermediate component in PE has been confirmed by NMR and Raman spectroscopy [14–17]. The relative proportion of the intermediate component in the amorphous phase of PE increases with increasing molar mass [18] and with increasing degree of chain branching [16]. Mutter et al. [19] suggested the existence of two different interphase components with similar characteristics to those of the liquid-like and crystalline components, respectively. Murthy et al. [20–22] have very recently explored the possibility of characterising the structure in noncrystalline regions, i.e. the local fluctuations in the average density and orientation of the amorphous chains by analysing the distribution of gases and liquid in a polymer. This approach may enable to us to use our additive as a probe molecule to show if it is possible to distinguish different zones in the amorphous regions.

The effect of some solvents on PA-12 and other polyamides has been investigated in numerous papers [23–27]. However there are only few studies on the solubility of substances of larger size like additives, which are usually solid substances at room temperature [28]. Since the knowledge of the solubility of a particular substance in a polymer is a fundamental issue that determines the state of the additive in a processed sample and the mechanism by which it may diffuse through the polymer and may be lost [29], the investigation of the solubility of erucamide in PA-12 is a point of primordial interest and a goal of this paper.

2. Experimental

2.1. Materials

2.1.1. Poly(laurolactam) (nylon 12) (PA-12) ($-[-(CH_2)_{11}-CO-NH-]_n-$)

The polymeric material was commercially available grade Vestamid L2106 F Natural free-additives supplied by Hüls Española, S.A. (Barcelona, Spain), a subsidiary Spanish company of Chemische Werke Hüls, A.G. Germany.

The intrinsic viscosity $[\eta] = 119.2\ \mathrm{ml\ g^{-1}}$ was determined in sulphuric acid (96%) at 298.2 K using a modified dilution Ubbelohde type of suspended level capillary viscometer. The weight-average molecular weight $\bar{M}_w = 1.13 \times 10^5$ g ml ($\overline{DP}_w = 575$) was determined viscometrically using the Mark–Houwink–Sakurada equation of Tuzar et al. [30] in sulphuric acid at 298.2 K:

$$[\eta] = 6.94 \times 10^{-2} \bar{M}_w^{0.64} \qquad (\mathrm{ml\ g^{-1}}) \tag{1}$$

2.1.2. Erucamide (13-cis-docosenamide) [$H_3C-(-CH_2-)_7-HC{=}CH-(-CH_2-)_{11}-CO-NH_2$]

A commercial sample of ARMOSLIP (EXP) beads with a 96.5% purity, which has been used in blends and as standard material for CGLC testings and calibrations, was kindly supplied by Akzo Chemicals, S.A. División Química, (El Prat de Llobregat, Barcelona, Spain) and used as received. Its melting point determined by DSC at a heating rate of 20 K $\mathrm{min^{-1}}$ was 359 K. A Perkin–Elmer DSC 7 calorimeter was used. The temperature scale was calibrated with purified naphthalene and biphenyl (mp 353.5 and 342.4°C, respectively).

2.1.3. Stearic acid

Stearic acid of 99% purity (Fluka Chemie, A.G. Buchs/Switzerland), employed as an internal standard was used as received.

2.1.4. Chloroform

An analytical grade chloroform (Quimicen, S.A., Madrid, Spain) needed for Soxhlet solvent extraction was used as received.

2.2. Methods

2.2.1. Preparation of mixtures

Blends of erucamide/PA-12 were prepared by mechanical blending in a home-made Brabender mechanical blender equipped with a mixing head of 50 ml capacity Rheomix 600 at 463 K and 24 rpm for 5 or 7 min and slowly cooled down to room temperature. Samples of unblended PA-12 and eru were subjected to the same treatment, i.e. same blending time, thermal history and percentage of antioxidant. Bubble-free films were prepared by compression moulding using a Collin Press Model 300 and then subjected to the following procedure: first, the sample in the form of

Table 1
Melting points T_m, apparent melting enthalpies, ΔH_m, of PA-12 and erucamide (*ERU I* and *ERU II*) and their blends measured by DSC at a heating rate of $R_H = 20.0$ K min^{-1}

Sample	Composition (wt% erucamide)	ρ (g ml^{-1})	First heating cycle						Second heating cycle					
			PA-12			Crystalline erucamide			PA-12			Crystalline erucamide		
			T_m (K)	ΔH_m (J g^{-1})	X_c (%)	$T_{m\,ERU\,I}$ (K)	$T_{mERU\,II}$ (K)	$\Delta H_{m(ERU\,I+ERU\,II)}$ (J g^{-1})	T_m (K)	ΔH_m (J g^{-1})	X_c (%)	$T_{mERU\,I}$ (K)	$T_{mERU\,II}$ (K)	$\Delta H_{m(ERU\,I+ERU\,II)}$ (J g^{-1})
1	–	1.015	444	64	31	–	–	–	443	68	32	–	–	–
2	1.5	1.014	447	63	30	–	–	–	444	61	29	–	–	–
3	3	1.014	445	63	30	–	–	–	444	64	30	–	–	–
4	6	1.007	446	63	30	–	–	–	442	68	32	–	–	–
5	13	1.009	445	65	31	355	336	40	440	72	34	352	338	47
6	29	0.999	442	66	32	358	342	85	436	80	38	353	343	87
7	38	0.991	435	69	33	357	341	115	434	78	37	355	345	112
8	100		–	–	–	359	–	143	–	–	–	359	–	144

pellets was heated up to 483 K and at a pressure of 5 bar was applied during 3 min. Immediately afterwards, the pressure was increased to 100 bar and held during 5 min. Finally the sample was quenched between two plates refrigerated with cool water (283 K) and at a pressure of 120 bar during 5 min. The films were vacuum dried at 323 K and 2×10^{-3} mmHg during 48 h to eliminate water.

2.2.2. Measurement of PA-12 and erucamide contents

The general analytical approach chosen was to extract the blends [1]. For eru content a method based on capillary gas–liquid chromatography (CGLC) has been followed. We have used a procedure reported by Brengartner [31] for the separation of fatty acid amides using glass capillary columns. Some other details and description of the chromatographic equipment and techniques have been given elsewhere [1]. Erucamide percentages for blends are included in the second column of Table 1.

2.2.3. Density measurement and degree of crystallinity

The density of pure PA-12, measured by means of a flotation and pycnometric technique, was 1.014 g cm^{-3}. The degree of crystallinity can be calculated by means of the following expression:

$$X_c = (1-\lambda)_d = \frac{\rho_c}{\rho}\frac{(\rho-\rho_a)}{(\rho_c-\rho_a)}100\% = \frac{(1/\rho_a)-(1/\rho)}{(1/\rho_a)-(1/\rho_c)}100\% \quad (2)$$

where ρ is the density of the sample, ρ_a the density of the whole amorphous PA-12 and ρ_c of the whole crystalline, namely, a sample 100% amorphous or crystalline, respectively.

In the literature there are some discrepancies in the values of the density for the amorphous and crystalline PA-12 [32,33]. As a result, it is not possibe to obtain accurate value for the degree of crystallinity from these data. By taking, from Table 1, a value of 1.0148 g cm^{-3} for the PA-12 density, we may say that the value of X_c may oscillate from 25% if the density of the amorphous and crystalline regions are assumed to be 0.996 and 1.077 g cm^{-3}, respectively [32] and 45% if the density of the amorphous and crystalline regions are assumed to be 0.99 and 1.048 g cm^{-3}, respectively [33]. Even so, this value agrees quite well with the one calculated from DSC measurements of 31% on a sample with almost the same thermal history, as can be seen in Table 1. Small differences in the density values of 100% amorphous or crystalline PA-12 may lead to quite noticeable differences in crystallinity.

A coarse estimation of X_c of PA-12 was also done from WAXS curves. Crystallinity was obtained drawing a straight baseline between 12 and 35° 2θ and then fitting a scaled amorphous curve under the diffraction peaks. The ratio of the areas of the crystalline peaks to the total area was taken as a weight fraction or index for the X-ray

crystallinity. It amounted to be 35%. This value agrees quite well with the one estimated from DSC measurements.

2.2.4. Differential scanning calorimetry

Differential scanning calorimetry (DSC) measurements were carried out under a blanket of N_2 with a Perkin–Elmer DSC-7 connected to a cooling system. In order to destroy the self-seeding nuclei in the components and to submit all the samples to the same thermal history; the samples were preheated at a rate of 20.0 K min^{-1} until 483 K and then crystallised at a standard rate of 10 K/min. Reheating runs were performed at a standard rate of 20.0 K/min. Typical sample weights ranged from 5 to 10 mg.

The melting temperatures were obtained from the endothermic maxima. The apparent melting enthalpy ΔH_m of unadditivated PA-12, pure erucamide and their blends were calculated from the area of the DSC endothermic peaks by using the indium melting enthalpy, $\Delta H_m(\text{indium}) = 28.46$ J g^{-1} as a standard. A detailed analysis of some of these endothermic peaks will be shown later on. The crystalline and amorphous weight fractions, after weight normalisation, were calculated from the following relations: $w_c = \Delta H_m/\Delta H_{PA-12}$ and $w_a = (1 - w_c)$, where $\Delta H_{PA-12} = 209.2$ J g^{-1} is the melting enthalpy per gram of 100% crystalline PA-12 [34].

2.2.5. Wide-angle X-ray scattering

Wide-angle X-ray diffraction patterns (WAXS) were taken by using a Geiger counter X-ray diffractometer made by Philips that used Ni-filtered CuK_α radiation. The generator operated at 40 kV and 25 mA. The intensities were recorded from 3 to 35 2θ degrees. The goniometer was calibrated with a standard of silicon. The X-ray diffractograms were normalised to the same total intensity after considering a flat background extending between 3 and 35 2θ degrees.

2.2.6. Dynamic mechanical measurements (DMTA)

Dynamic mechanical relaxations were measured with a Polymer Laboratories MK II Dynamic Mechanical Thermal Analyser, working in the tensile mode. The storage modulus E', the loss modulus E'' and the loss tangent, tan δ, of each sample were obtained as functions of temperature over the range from 123 to 400 K at fixed frequencies of 1, 3, 10 and 30 Hz and at a heating rate of 1.5 K min^{-1}. Blend strips from sheets were cut around 200–300 μm thick using a die 2.2 mm wide and 1–2 cm length. The specimens corresponding to samples with high eru content do not have enough mechanical strength to carry out dynamic mechanical measurements in the tensile mode. There exist a series of procedures for measurements which include impregnating the sample on thin metal strips [35–37], glass braid, glass filter mat, or cellulose mat supports [37]. Therefore, those samples were coated on aluminium after checking the dynamic mechanical inactivity of the support in the temperature range studied.

The apparent activation enthalpy values were calculated according to an Arrhenius-type equation, considering an accuracy of ±1 K in the temperature assignment from the maxima.

3. Experimental results

3.1. Differential scanning calorimetry

Fig. 1 displays the melting behaviour of PA-12, pure erucamide and their blends, from 300 to 473 K at a heating rate of 20 K min^{-1} in the second heating cycle. It is only possible to distinguish the endotherm corresponding to the melting of PA-12 and at lower temperature two endotherms corresponding to the melting of eru. In Table 1 the T_m calculated from the maximum of these endotherms and melting enthalpy ΔH_m corresponding to the first and second heating cycle are summarised in order to compare with the X-ray and DMTA results. For the samples with the lowest eru content (1.5, 3 and 6%) only a peak corresponding to the melting of PA-12 occurs, indicating that eru is dissolved in the amorphous regions of PA-12. However the T_m of PA-12 does not depend on the composition for these samples and it decreases only for samples with higher erucamide content. This fact points out that the eru does not act as a diluent for PA-12, i.e. by depressing its melting point.

As can be very easily seen in Fig. 2, for samples with 13, 29 and 38% of erucamide two overlapped endotherms are observed at the melting region of erucamide which were also reported in a previous publication [5] for erucamide/i-PP blends. In this early case, the sharp endotherm appearing on the right side was assigned to crystalline eru supported on the external surface of i-PP as globules, or droplets, and it was designated as external eru (*ERU I*). The endotherm appearing at the lowest temperature side (around 335 K) was assigned to eru located in the amorphous regions of i-PP which surrounds the spherulites and/or in the amorphous regions inside the spherulites (*ERU II*). The melting enthalpy of *ERU II* ($\Delta H_{m(ERU\ II)}$) could be calculated taking into account the melting enthalpy of *ERU I* ($\Delta H_{m(ERU\ I)}$) which is the same as for pure erucamide (144.2 J g^{-1}). The value obtained was $\Delta H_{m(ERU\ II)} = 78.6$ J g^{-1} [5].

As in our previous work, the traces could be resolved and the area of each endotherm calculated by means of a curve deconvolution method. Once the area was known it was possible to estimate the amount of *ERU I* and *ERU II* by using the $\Delta H_{m(ERUI)}$ and $\Delta H_{m(ERUII)}$. The amount of erucamide left corresponds to the amorphous erucamide dissolved in the amorphous regions of PA-12. This erucamide will be referred as *ERU III*. If we assume that *ERU III* is exclusively dissolved in the amorphous regions of PA-12, it will be proportional to the amount of these regions.

It is possible to correlate the amount of eru dissolved and crystallised in the amorphous regions with the amount of

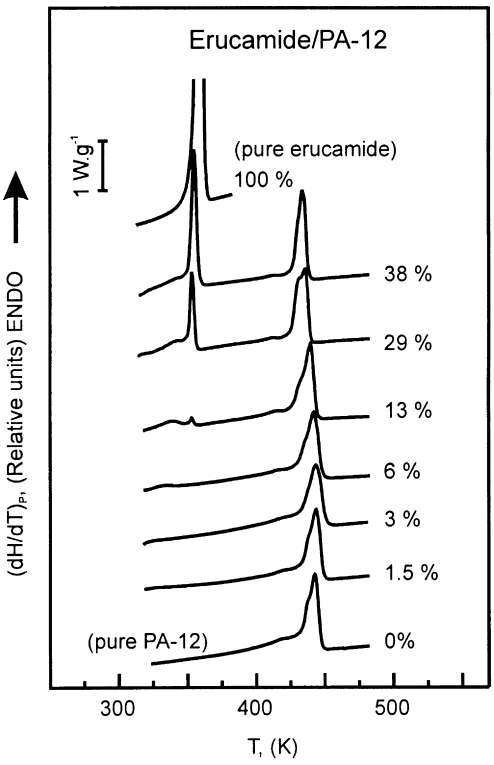

Fig. 1. DSC grams recorded during a second heating cycle at a nominal heating rate of $R_H = 20.0$ K min^{-1}, for PA-12 and a series of erucamide/PA-12 blend crystallised under the same thermal history, i.e. melting from 303 to 483 K at a rate of heating of $R_H = 20.0$ K min^{-1}, 5 min at 483 K and then cooled down to 303 K at a rate of cooling of $R_C = 10$ K min^{-1}. Their compositions are indicated.

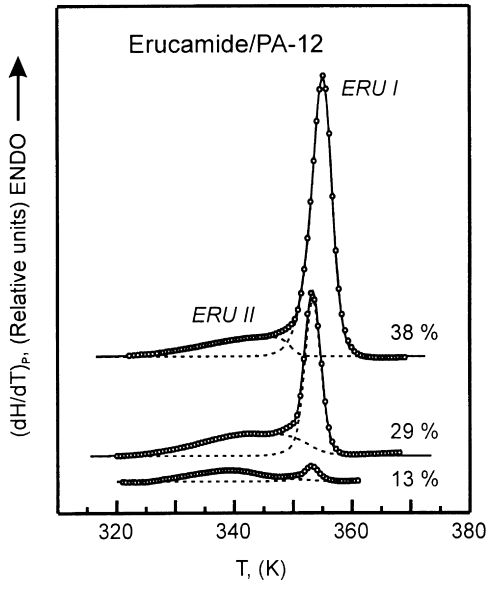

Fig. 2. Deconvolution of some of the DSC grams in the erucamide region of a series of erucamide/PA-12 blends as shown in Fig. 1. Their compositions are indicated.

amorphous content in PA-12. Thus for instance, in Fig. 3, ratios of *ERU I*, *ERU II* and *ERU III* to the PA-12 amorphous content, are plotted as a function of the eru content (wt%) in the blend. This plot has been done to correct the molecular species content (*ERU I*, *II* and *III*) with respect to the degree of crystallinity with the intent to not only show the dependence of each of these molecular species of eru on the blend composition but also test phenomenologically our hypothesis about the localisation of the three different species present in erucamide/PA-12 blends. As it can very easily seen in this plot, at the beginning, eru molecules occupy only the region of the liquid-like amorphous component until a constant level of eru is attained, then eru molecules begin to be distributed among the properly named amorphous region and start to form the microdomains or droplets, *ERU I*, in the polymeric matrix. The level of *ERU II* attains a constant value whereas the amount of erucamide as microdomains or droplet almost grows exponentially as a function of the erucamide content in the blend. In other words, *ERU II* and *ERU III* species are directly proportional to the percentage of amorphous part of PA-12 in the blend. Just below approximately a 6% erucamide content blend, erucamide molecules are dissolved in the liquid-like component of the amorphous regions of PA-12, occupying about a maximum of 10% of this part. When the erucamide content in the blend increases, a part of erucamide is crystallised in the amorphous regions with segmental mobility in between crystalline and crystal-like zones as *ERU II* until almost 27% of it contains *ERU II*. When the amorphous regions cannot accommodate more erucamide, this will be segregated and will crystallise forming globules or droplets outside of both amorphous regions (polymeric matrix).

3.2. Crystallinity

Values for the PA-12 crystallinity X_c in erucamide/PA-12 blends are given in the sixth column of Table 1. As it can be seen, the degree of crystallinity does not seem to depend appreciably on the erucamide content. Only for the samples with 29 and 38% of erucamide X_c increases but almost in the range of the experimental errors. This fact and the increase of T_m for these two samples point out that erucamide induces only a slightly increase of the crystallisation in PA-12, which cannot be taken into account to explain any type of influence of this property on some characteristics and behaviour of the blends.

3.3. Wide-angle X-ray scattering

The crystalline structure of PA-12 has been investigated by several authors [38–46]. PA-12 exhibits the γ-form as its stable structure. The unit cell is monoclinic. In Fig. 4 the WAXS curves for eru, PA-12, and their blends are shown. In the spectra of the blends there only appear the characteristic diffraction maxima due to each one of the pure components. Thus, for PA-12 you can see the reflection corresponding to

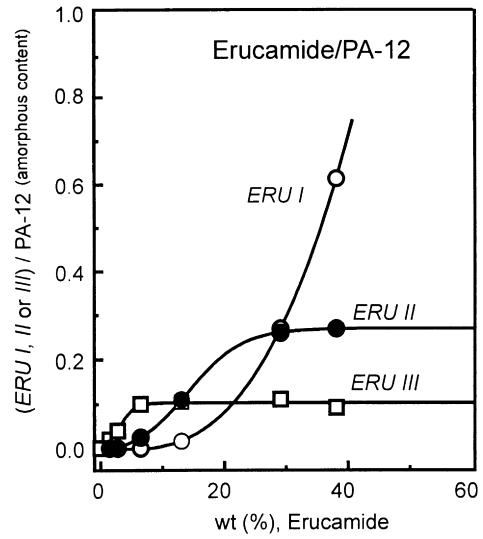

Fig. 3. Plot of the proportion of each erucamide type (*ERU I*, *II* and *III*) in the amorphous regions of PA-12 as a function of the erucamide content in the sample (wt%). They have been calculated as indicated in the text.

the γ-form. The reflections corresponding to erucamide are not observable until the sample with a 29 wt% of eru. We did not observe any changes in the position of the reflections in the blends. Because of this it is possible to conclude that the crystallisation of both components takes place separately.

3.4. Dynamic mechanical measurements

Before going into the DMTA experimental results, it is quite convenient to make some comment that water exerts a considerable influence on PA-12 relaxations [25]. Kollross and Owen [33] have studied the influence of hydrogen bonding on the mechanical behaviour of PA-12. The presence of water may affect the position, height and broadening of the relaxations as follows [25]: (a) The temperature of the α peak decreases by ca 20 K and its height, in general, remains essentially unchanged. (b) The temperature of the β peak remains unaffected, but its height increases by about a factor of two. (c) The temperature of the γ peak may be decreased by 3–5 K; its height remains unaffected but the peak becomes narrower. For this reason, the samples were vacuum-dried as explained in Section 2.

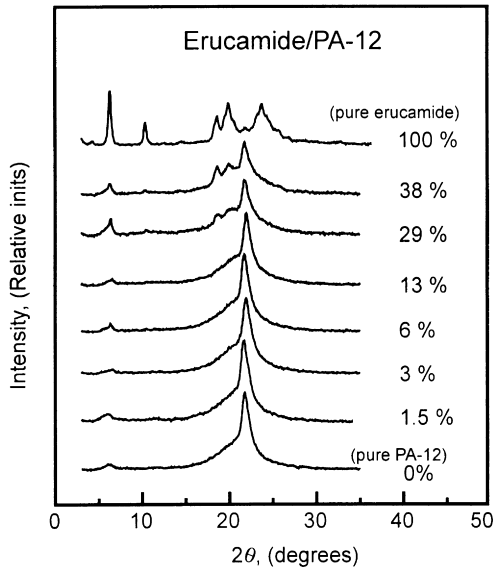

Fig. 4. WAXS of PA-12 and erucamide and their blends. Their compositions are indicated.

Fig. 5 shows the loss tangent tan δ against temperature *T* at 3 Hz for PA-12, pure erucamide and their mixtures. As it can be seen the three well-known relaxations for polyamides [25,47–50] are present. The α-relaxation corresponding to the glass transition and at the lowest temperature the γ-relaxation appears arising from kink and crankshaft motions of a sequence higher than four methylene groups. Between these two relaxations, the β-relaxation occurs and it is related to carbonyl groups forming hydrogen bonds in the amorphous regions. Small amount of water has a large influence on this relaxation [25].

At higher temperature than the α-relaxation, around 370 K, a peak of low intensity appears that was also observed for PA-6 and attributed to the crystalline regions. However, Khanna [51] studied a PA-6 sample annealed during long time at high temperature in order to avoid prefusion and recrystallisation processes. He observed a broad relaxation at 443 K by mechanic dynamical analyses that was attributed to movements of interfacial amorphous regions, whereas Varlet et al. [25] suggested a change in the crystal form for the PA-12.

In pure erucamide three relaxation regions appear, namely α-, β- and γ-relaxations. We believe that the β- and γ-relaxations have the same origin as in polyamides, but the α-relaxation due to the closeness of the melting point of erucamide was attributed to a premelting process [4].

The tan δ for mixtures shows the three relaxation processes observed for the pure components. The relaxation maxima for erucamide and pure PA-12 are very close, only the temperature of the α-relaxation of erucamide is slightly higher than the one for PA-12 and its origin is also different. It is in the region of the α-relaxation of PA-12 that the effect of the composition is more pronounced.

The temperatures of the maximum for α-, β- and γ-relaxations at 3 Hz for PA-12, pure erucamide and their mixtures are collected in Table 2 as well the apparent activation energy E_a of the processes. E_a was calculated from the frequency shift of the relaxation temperature and assuming that it follows an Arrhenius process. The α-relaxation corresponding to the T_g involves more cooperative motions than the other two relaxations as confirmed by a much higher activation energy. The activation energy for the γ-relaxation lies in the range found experimentally as well as by conformational dynamics calculations [52].

Whereas the E_a of the γ- and β-relaxations remains unaffected by the composition, E_a of the α process increases

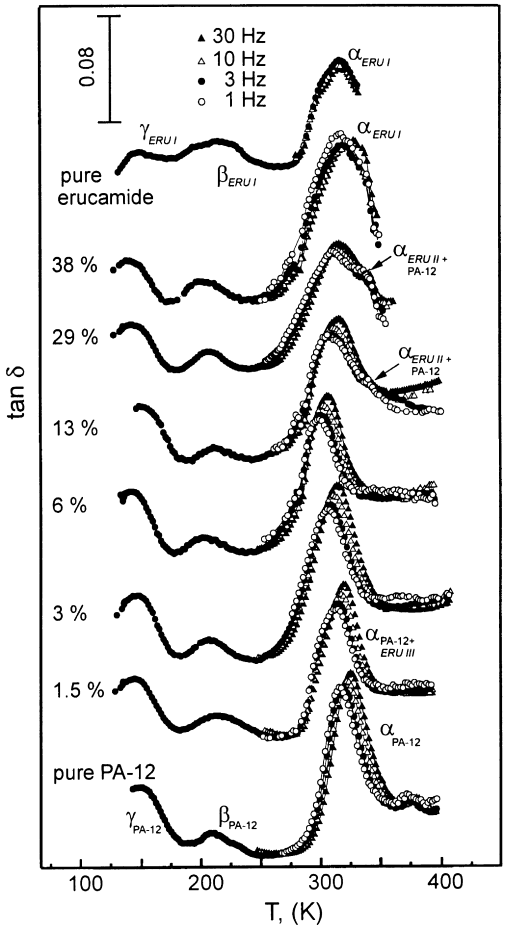

Fig. 5. Dynamic mechanical loss tangent (tan δ) at 3 Hz as a function of temperature for a series of erucamide/PA-12 blends. Erucamide content of the blends are indicated.

with increasing the erucamide content approaching the E_a value for the α-relaxation of pure erucamide. At this point it is worth noting that when the values of the activation energy $E_a > 400$ kJ mol^{-1} the error in its estimation is considerably high, however they have been gathered in Table 2 only for comparative purposes.

In Fig. 6, as it can be seen, the temperature (T_g) of the maximum T_{max} of tan δ of the α-relaxation decreases with increasing erucamide content until the 6% sample, in fact the glass transition temperature T_g decreases from 320 to 304 K, namely 16 K for a composition from a 0% to around a 6% of erucamide content. At the same time the intensity of the α-relaxation decreases. After this composition the temperature of the maximum increases approaching the temperature of the α-relaxation for pure erucamide. For higher erucamide-content samples, the relaxations broaden and existence of two relaxations is very clearly seen: one which corresponds to PA-12 and the other to erucamide. This fact is in agreement with the DSC and X-ray diffraction results at concentrations where the phase separation becomes apparent.

The temperature of the onset of α-relaxation T_{onset} was also investigated. Fig. 6 also displays T_{onset} against the proportion of eru in the sample. T_{onset} decreases strongly with increasing erucamide content until the 6% of erucamide in the sample is reached, for higher content the T_{onset} remains unaffected.

In Fig. 7, the values of the storage modulus E' at three selected temperatures are plotted against the blend erucamide content. It shows the fall of E' for blends with an eru content lower than 13 wt%. For higher eru contents its behaviour could seem to be unusual and it will be discussed in the next section.

4. Discussion of results

A number of similarities have been found when comparing the behaviour of the present system with that one of the previously investigated erucamide/i-PP. Erucamide/i-PP blends were studied using DSC, WAXS, polarised optical microscopy, scanning electron microscopy (SEM) [5], DMTA, dielectric thermal analysis (DETA) [4], solid state NMR spin diffusion experiments and two-dimensional (2D) ^{1}H–^{13}C-NMR [6]. Erucamide/i-PP blends showed a characteristic behaviour typical of incompatible systems. DSC studies have demonstrated that the crystallisation of

Table 2
Dynamic mechanical relaxations of PA-12, pure erucamide and a series of their blends measured at 3 Hz

Sample	Composition (wt% erucamide)	T (K)					
		γ		β		α	
		3 Hz	E_a (kJ mol^{-1})	3 Hz	E_a (kJ mol^{-1})	3 Hz	E_a (kJ mol^{-1})
1	0	149	46	211	75	320	351
2	1.5	145	50	215	71	315	364
3	3	146	46	208	71	309	313
4	6	142	50	205	63	304	364
5	13	146	46	207	54	307	313
6	29	144	46	210	75	315	456
7	38	142	46	204	67	321	468
8	100	151	71	214	180	317	773

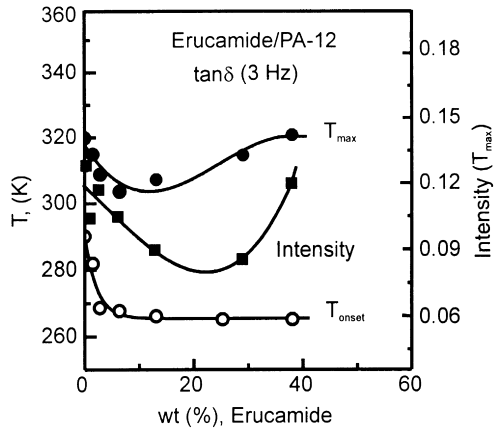

Fig. 6. Plot of the temperature of tan δ maxima (T_{max}) and onset temperature (T_{onset}) and intensity of the α-relaxation (at 3 Hz) of the dynamic mechanical curve as a function of the erucamide content (wt%) for PA-12 and a series of erucamide/PA-12 blends.

erucamide/i-PP blends results in separated crystals of the two components rather than co-crystallisation. The melting temperature of i-PP did not depend on the erucamide composition in the blends. The apparent melting enthalpies were also unaffected by the composition. However, for low erucamide-content blends, DSC traces revealed two endothermic transitions. The lower one was assigned to erucamide crystallised inside the amorphous regions of i-PP, and the higher one to erucamide segregated from the i-PP matrix which is crystallised with the same structure as pure crystalline erucamide. Most of the segregated erucamide forms a second phase as globules or droplets, and therefore only a minor part is located in the amorphous regions of the i-PP spherulites. Similarly, the dynamical

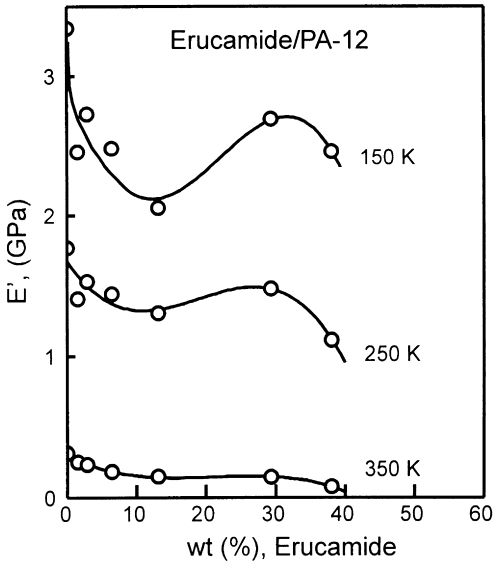

Fig. 7. Plot of the dynamic storage modulus (E') at several temperatures (150, 250 and 350 K) as a function of the erucamide content (wt%) for PA-12 and a series of their blends with erucamide.

mechanical and dielectric relaxations of these blends did not vary substantially with the morphology, thus it was suggested that the amorphous phase of spherulites has a constant composition.

In the present paper, a quite similar behaviour to the erucamide/i-PP system reported previously [4] has been found. However erucamide/PA-12 blends have shown a better compatibility [3]. Thus, for erucamide contents lower than 6%, DSC grams did not show any endotherm trace. This fact may be indicative that erucamide molecules are in the amorphous state in these blends. However, for erucamide contents higher than 6%, erucamide may crystallise in two different crystalline forms, probably depending upon the morphological structure of the guest polymer, i.e. the matrix in each one of the cases. There exist two possibilities of location for crystalline erucamide as in the case of erucamide/i-PP blends, namely in the amorphous regions of PA-12 forming a heterogeneous phase as well as a heterogeneous segregated phase where the erucamide molecules are crystallised forming a dispersed phase as microdomains or droplets phase and therefore outside the amorphous regions. Erucamide acts as a plasticiser for PA-12, until a 10% erucamide content is dissolved in its amorphous regions. Erucamide can form hydrogen bonds between one or two PA-12 chains increasing the local volume. However the plasticizing effect is not notable as proved by the slightly decreasing of the α-relaxation temperature of PA-12. The decreasing of the T_{onset}, yielding constant values for higher erucamide content than 6% is related to a constant composition of the plasticised amorphous phase of PA-12.

The storage modulus may either increase or decrease with the addition of a plasticiser and indeed the modulus behaviour can change depending upon the amount of platiciser added. The dynamic mechanical spectrum of the polymer plus plasticiser can be different from that of the pure polymer [53]. As it can be seen in Fig. 7, the storage modulus E' decreases as the erucamide content in the blend increases until a percentage of the 6% is attained. There exist probably some plausible explanations for the dependence of storage mechanical modulus on blends composition shown in Fig. 7. Since in this case the additive molecules (*ERU III*) act as a plasticiser of the polymer due to its compatibility, and the polymer repeating units are almost similar structurally to additive molecules, repeating unit should also interact with molecules of the additive. It is the higher mobility of the diluent that allows for improved packing and therefore the formation of structures with a favourable interaction. In fact, we have two effects, one due to the plasticisation and the other which promotes an increasing of the intrachain and interchain interactions and therefore the modulus. Both effects work in opposite direction and are represented by a balance, so the trend represented in Fig. 7 at 150 K. Firstly, when a concentration of the additive from 0 to 12–14% is used, an effect typical of a plasticiser is observed. Secondly, between 14 and 32%, an increase of the interactions in the blend must

play an important role and therefore causing an increase in the modulus. In the third place, namely concentrations higher than 32% of additive in the blends, the effect of the additive fundamentally acts as an inactive filler because its droplet structure slowing down again the modulus. This mechanism is strongly temperature dependent as it could be expected, i.e. the higher the temperature the lower the effect, as it is shown by the data at 350 K. In favour of these assumptions, Bessler and Bier [54] by means of FTIR have shown that over 99% of the –CONH– groups in aliphatic dry polyamides are H-bonded at room temperature. Increasing the temperature from 30 to 210°C (i.e., well above the α and β peaks temperature) for PA-11 [55] does not significantly modify the percentage of free –NH–. The predominant effect of increasing the temperature seems to be a reduction of the average strength of the H-bonds between –CONH– groups [54,55]. However, Serpe and Chaupart [28] have shown that the percentage of free –NH– groups in PA-11, plasticised or not, is much lower than 1% at room temperature and increases slowly with temperature to reach 10–15% at 260°C. Increasing temperature leads to a reduction of the average strength of H-bonded –CONH– groups, which facilitates exchange of H-bonding partners.

There may exist another possibility to explain the E' behaviour shown in Fig. 7 based in part on changes of PA-12 crystallinity observed as a function of the composition. However this alternative has to be ruled out because the small changes observed in the values of ΔH_m cannot be enough to explain such a dependence.

In Fig. 5 it is seen that for blends with compositions higher than 6% by weight, there is a shoulder around 340 K on the right-hand side of the α-relaxation. However, this shoulder is clearly shown for the 29 wt% blend it is not easily detected in the 13 wt% blend. For the 38 wt% blend the relaxation not only broadens but also its intensity increases and it is still possible to detect the shoulder on the right hand side. The origin of the relaxations found in this region is also clearly seen if we have a detailed look at the intensity of the maxima from the curves obtained at different frequencies. The intensity of the α-relaxation of PA-12 increases with frequency as it is usual with many other polymers when this relaxation is associated to the amorphous phase and more precisely to the glass transition temperature T_g. On the contrary, in the case of pure erucamide, the intensity of the relaxation is higher at lower frequencies. This may be indicative of the different origin of this relaxation and that it can be due to motions of the crystalline regions. A similar behaviour associated to the crystalline phase has been found in the case of PE or in PP.

The deconvolution of this broad peak into their individual contributions from the different relaxations taking place is not possible. However they can be analysed qualitatively. Until a blend with a 6 wt% eru composition it is very clear that plasticisation of PA-12 is the only relevant effect observed as it put forward by the decreasing of both, the glass transition temperature T_g and the storage modulus E'. For the blend with a 13 wt% eru content, the plasticizing effect is maintained but at the same time eru starts to crystallise in the amorphous regions of the PA-12 which have been denominated as "*intermediate component or disordered phase of anisotropic nature*". The shoulder around 340 K agrees with the melting endotherm of *ERU II*. This fact moves us to assign it to a relaxation induced by the melting of erucamide located in the stiff amorphous regions of PA-12. This relaxation becomes most evident for the blend with 29 wt% erucamide content, which in turn is the blend where the *ERU II* content is higher. For this sample an increase of the maximum temperature is observed. It is may be attributed fundamentally to the T_g which is in agreement with the filler effect of *ERU II* observed by the increase of the storage modulus E'. When the content of eru in blends is augmented to a 38 wt%, the dominant process is the relaxation corresponding to the crystalline regions of eru in droplets or microdomains (*ERU I*), as it is demonstrated by the change in intensity when tan δ is measured at different frequencies, i.e. the intensity decreases as the frequency is increased as in the case of pure eru.

5. Conclusions

- Differential scanning calorimetry (DSC), wide angle X-ray scattering (WAXS) and dynamic mechanical analysis (DMTA) have been used to investigate the effect of a low molecular weight additive (erucamide) blended with poly(laurolactam) (PA-12).
- A good compatibility has been found for blends with low erucamide content as proved by the disappearance of the melting endotherm of erucamide and the decrease of the temperature of the α-relaxation (T_g) of PA-12 with increasing composition until the sample of 6 wt% of eru. At these concentrations, the additive acts as a plasticiser. This amorphous region may be denominated as "*melt-like or liquid-like amorphous component*".
- For higher erucamide content than 6 wt%, an endotherm corresponding to erucamide crystallised in the amorphous regions appears. The erucamide dissolved in the amorphous regions (*ERU III*) and the erucamide crystallised in the amorphous regions (*ERU II*) are proportional to the amorphous fraction of PA-12. This second amorphous region may be denominated as "*intermediate component or disordered phase of anisotropic nature*".
- For high erucamide content blends, eru is segregated outside the amorphous regions and crystallites as pure erucamide.

Acknowledgements

This work was funded in part by a grant from the DCICYT through Grant PB-95-0134-002-00. One of us

(I.Q.-G.) wishes to acknowledge to the Consejeria de Educación of the Comunidad Autónoma of Madrid for a maintenance grant Beca for Formación del Personal Investigador y Técnico of the Plán Regional de Investigación.

References

[1] Quijada-Garrido I, Barrales-Rienda JM, Frutos G. Macromolecules 1996;29:7164–76.
[2] Quijada-Garrido I, Barrales-Rienda JM, Alejo Espinoza L, Fierro JLG. Macromolecules 1996;29:8791–7.
[3] Quijada-Garrido I, Fernández de Velasco-Ruiz M, Barrales-Rienda JM. Macromol Chem Phys 2000; in press.
[4] Quijada-Garrido I, Barrales-Rienda JM, Pereña JM, Frutos G. J Polym Sci B: Polym Phys 1997;35:1473–82.
[5] Quijada-Garrido I, Barrales-Rienda JM, Frutos G, Pereña JM. Polymer 1997;38:5125–35.
[6] Quijada-Garrido I, Wilhelm M, Barrales-Rienda JM, Spiess HW. Macromol Chem Phys 1998;199:985–95.
[7] Peterlin A. J Macromol Sci 1975;B11:57–87.
[8] Billingham NC. In: Pospisil P, Klemchuck PP, editors. Oxidation inhibition in organic materials, 2. Boca Raton, FL: CRC Press, 1990 chap. 6, p. 249.
[9] Hildebrand JH, Scott RL. The solubility of nonelectrolytes, 3. New York: Reinhold, 1950.
[10] Stannett V, Yasuda H. In: Raff RA, Doak KW, editors. Crystalline olefin polymers, New York: Interscience, 1964 Part II, chap. 4, p. 131.
[11] Földes E. Deg Estab 1995;49:57–63.
[12] Hudson SD, Davis DD, Lovinger AJ. Macromolecules 1992;25:1759–65.
[13] Hedenqvist M, Gedde UW. Prog Polym Sci 1996;21:299–333.
[14] Kitamaru R, Horii F, Murayama K. Macromolecules 1986;19:636–43.
[15] Kitamaru R, Horii F, Hyon S-H. J Polym Sci: Polym Phys Ed 1977;15:821–36.
[16] Mandelkern L, McLaughlin KW, Alamo RG. Macromolecules 1992;25:1440–4.
[17] Strobl GR, Hagedorn W. J Polym Sci: Polym Phys Ed 1978;16:1181–93.
[18] Frisch HL, Stern SA. CRC critical reviews in solid state and materials sciences, 11. New York: Academic Press, 1976.
[19] Mutter R, Stille W, Strobl GR. J Polym Sci Part B: Polym Phys 1993;31:99–105.
[20] Murthy NS, Akkapeddi MK, Orts WJ. Macromolecules 1998;31:142–52.
[21] Murthy NS, Minor H, Bednarczyk C, Krimm S. Macromolecules 1993;26:1712–21.
[22] Murthy NS, Correale ST, Minor H. Macromolecules 1991;24:1185–9.
[23] Knopp B, Suter UW. Macromolecules 1997;30:6114–9.
[24] Starkweather HW, Barkley JR. J Polym Sci: Polym Phys Ed 1981;19:1211–20.
[25] Varlet J, Cavaillé JY, Perez J, Johari GP. J Polym Sci Part B: Polym Phys 1990;28:2691–705.
[26] Pathmanathan K, Cavaillé JY, Johari GP. J Polym Sci Part B: Polym Phys 1992;30:341–8.
[27] Le Huy HM, Rault J. Polymer 1994;35:136–9.
[28] Serpe G, Chaupart N. J Polym Sci Part B: Polym Phys 1996;34:2351–65.
[29] Billingham NC. Makromol Chem Makromol Symp 1989;27:187–205.
[30] Tuzar Z, Bohdaneckú M, Puffr R, Šebenda J. Eur Polym J 1975;11:851–5.
[31] Brengartner DA. J Am Oil Chem Soc 1986;63:1340–3.
[32] Andersson P. Makromol Chem 1976;177:271–7.
[33] Kollross P, Owens AJ. Polymer 1982;23:829–33.
[34] Gogolewski S, Czerniawska K, Gasiorek M. Colloid Polym Sci 1980;258:1130–6.
[35] Heijboer J. Kolloid Z 1960;171:7–15.
[36] Heijboer J. Polym Eng Sci 1979;19:664–75.
[37] Cowie JMG. Polym Eng Sci 1979;19:709–15.
[38] Khanna YP. Macromolecules 1992;25:3298–300.
[39] Prest WM, O'Reilly JM, Roberts FJ, Mosher RA. Polym Eng Sci 1981;21:1181–7.
[40] Dosière M. Polymer 1993;34:3160–7.
[41] Inone K, Hoshino S. J Polym Sci: Polym Phys Ed 1973;11:1077–89.
[42] Ishikawa T, Nagai S, Kasai N. Makromol Chem 1981;182:977–88.
[43] Gogolewski S, Czerniawska K, Gasiorek M. Colloid Polym Sci 1980;258:1130–6.
[44] Owen AJ, Kollross P. Polym Commun 1983;24:303–6.
[45] Northolt MG, Tabor BJ, Van Aarsten JJ. J Polym Sci Part A-2 1972;10:191–2.
[46] Cojazzi G, Fichera A, Garbuglio C, Malta V, Zannetti R. Makromol Chem 1973;168:289–301.
[47] McCrum NG, Read BE, Williams GW. Anelastic and dielectric effects in polymeric solids, New York: Wiley, 1967 chap. 12.
[48] Murayama T. Dynamical mechanical analysis of polymeric materials, New York: Elsevier, 1978.
[49] Rotter G, Ishida H. Macromolecules 1992;25:2170–6.
[50] Greco R, Nicolais L. Polymer 1976;17:1049–53.
[51] Khanna YP. J Appl Polym Sci 1990;40:569–79.
[52] Heaton NJ, Benavente R, Pérez E, Bello A, Pereña JM. Polymer 1996;37:3791–8.
[53] Liu Y, Roy AK, Jones AA, Inglefield PT, Ogden P. Macromolecules 1990;23:968–77.
[54] Bessler E, Bier G. Makromol Chem 1969;122:30–37.
[55] Skrovanek DJ, Painter PC, Coleman MM. Macromolecules 1986;19:699–705.